J. theor. Biol. (1993) **160**, 97–133

Cellular Automata Approaches to Biological Modeling

G. BARD ERMENTROUT AND LEAH EDELSTEIN-KESHET

Department of Mathematics and Statistics, University of Pittsburgh, Pittsburgh, PA 15260, U.S.A. and Department of Mathematics, University of British Columbia, Vancouver, BC V6T 1Z2, Canada

(*Received on* 27 *November* 1991, *Accepted on* 30 *June* 1992)

We review a number of biologically motivated cellular automata (CA) that arise in models of excitable and oscillatory media, in developmental biology, in neurobiology, and in population biology. We suggest technical and theoretical arguments that permit greater speed and enhanced realism, and apply these to several classical examples of pattern formation. We also describe CA that arise in models for fibroblast aggregation, branching networks, trail following, and neuronal maps.

1. Introduction

Modeling complex physical phenomena through computer simulations has become a common tool for understanding the natural world. Realistic models based on physical laws generally result in large systems of non-linear integro- and partial-differential equations. This is particularly true for biological phenomena. The "bottom-up" approach to modeling has many advantages, such as the ability to reproduce in quantitative detail the results of an experimental procedure. However, there is a price paid for such detail. It is often difficult to extrapolate the behavior of the "realistic" model to different experimental and natural conditions. These models sometimes obscure the basic physical principles underlying the modeled phenomena. A majority of complex biological systems cannot be precisely quantified so that detailed models may be premature. Finally, such models lead to formidable numerical problems that require huge memories on fast computers. Thus it becomes very difficult and time consuming to parametrically explore the system. One technique for simplifying these often numerically intractable systems is to mimic the physical laws by a series of simple rules that are easy to compute quickly and in parallel. We loosely call these simple systems cellular automata (CA). More properly, a cellular automaton consists of a simulation which is discrete in time, space, and state.

All results of computer experiments are in fact CA, since all computers operate at finite precision on numerical discretizations of the time and space domains. However, most CA simulations reduce the state space to only a few states (often as few as two) and subdivide time into discrete steps in a very simple fashion. Although there may at times be a fine line between a numerical simulation and a CA, the features which stem from the discrete nature of the system are not disguised in the latter. In contrast is the great care taken in many numerical algorithms (for solving ordinary differential equations, for example) to overcome the "artifacts" or spurious behavior owing to discretization.

0022-5193/93/010097+37 $08.00/0

CA have stirred great interest in physics, particularly in computational fluid dynamics (CFD). Two recent issues of *Physica D* (Farmer *et al.*, 1984, Gutwitz, 1990) have been devoted to CA with particular emphasis on abstract dynamics and physical applications. A recent book edited by Wolfram collects many articles from diverse sources on the behavior and applications of CA (Wolfram, 1986). At least one journal, *Complex Systems*, is primarily devoted to CA research. Rucker (1989) has created software for exploring a large variety of CA as well as producing new ones; he provides a nice historical introduction and many references to the field. Tofolli & Margolis (1988) have developed a hardware device for rapidly exploring simple two-dimensional rules. Most of the work by physicists has been to view the automata as abstract dynamical systems and then to characterize their behavior via calculation of entropy, complexity, and other quantitative measures of dynamics.

Biological systems are ripe for modeling with CA methods; the spatial and temporal patterns are diverse and fascinating. Our knowledge of the details of a particular mechanism is often full of gaps and, unlike physics, there are few "laws" such as the Navier–Stokes equations or Newton's laws. Thus, simplified models can be useful in precluding certain mechanisms as being impossible or at least unlikely. The speed by which calculations can be made allows the investigator to examine a huge number of parameter ranges that would be otherwise impractical for more "realistic" simulations. Because of their simplicity, it is often felt that CA models are nothing more than glorified computer games which are unable to provide any real insight into the biological phenomenon. We believe that this view is incorrect and in fact, qualitative (and sometimes quantitative) agreement between these simple models and experimental results can be had.

The purpose of this paper is to present some recent CA models that have arisen in our efforts to understand biological self-organization. We have complemented analytic partial differential equation models with a number of biologically motivated automata. Typically, our continuum models involve averaging out the spatial organization in order to obtain simplified and tractable equations. We describe a number of different approaches and compare these to approaches taken by other authors. Our main interest lies in using CA to examine spatial and temporal pattern formation.

We divide CA models into three broad classes: (i) deterministic or "Eulerian" automata; (ii) "lattice gas" models; and (iii) "solidification" models.

In a deterministic automaton, the spatial domain of the model is divided into a fixed lattice and each lattice point has a state associated with it. The state at the next time step is determined solely from earlier states of the cell and its neighbors. This type of automaton most closely resembles an evolution equation such as a partial differential equation or an integral equation. In section 3 we describe a number of such automata and how they mimic the real partial differential equations. Examples where this type of model is applicable include waves in excitable and oscillatory media, predator–prey models, and spatial pattern formation. We end section 3 with some recipes for constructing CA models from differential equations and apply these methods to an activator-inhibitor model.

Lattice gas models are also called particle systems and consist of a discrete spatial grid on which particles move about and interact in some prescribed fashion. Unlike the deterministic automata above, these systems are usually driven by random events. Thus, the same initial conditions will not yield identical final states except in some average sense. These models, by virtue of their probabilistic nature, suggest a mean field theory and certain differential equations that are themselves tractable. In section four, we describe models for fibroblast aggregation, self-organization of ant trails, and topographic neural maps.

A "solidification" model is much like a lattice gas model except that once a particle is in a "bound" state it can never move or disappear again. This type of model has been used to model phase-transitions (hence the name "solidification") and precipitation (Packard, 1986). We describe applications of this type of model to biological systems in section 5. Examples of behavior for which "solidification" models are appropriate include branching structures such as growth patterns of fungi, angiogenesis (formation of vascular networks), and growth of immotile colonies of bacteria under conditions of nutrient limitation.

2. Biological Cellular Automata

CA have sporadically appeared as simplified models for a variety of biological situations. A majority of these represent abstractions of partial-differential equations that purport to model the spatial and temporal patterns of the given phenomenon. Thus they fall under our classification of deterministic CA. We describe some of the applications for these models.

2.1. ACTIVE MEDIA

The best known examples of CA in biological or physiological literature are the "excitable media" which mimic the behavior of nerve cells, muscle cells, cardiac function, and chemical reactions. An excitable medium is one in which there is a unique stable rest state and such that small perturbations relax to this state. Sufficient perturbations (above threshold) lead to a large transient increase (the excited state) in some of the components before relaxing to the rest state (recovery). For a certain amount of time during the recovery period, the medium is unable to be re-excited regardless of the size of the perturbation (the refractory period.) Examples of this type of phenomena include axonal excitability, cell signaling, cardiac fibers, and many other physiological events.

Excitable CA attempt to reduce an excitable medium to its simplest possible form. Each cell in an excitable CA is connected to some fixed number of neighbors. The simplest excitable rule has three states 0, E, and R, representing the resting or zero state, the excited state, and the refractory state, respectively. If a cell is in E then at the next time step it becomes R and after that it is returned to 0. If a cell is in state 0 and at least one neighbor is in state E then at the next time step, the cell is put in state E. All modifications of excitable CA are based on this simple conceptual rule. One of the first examples of this type of automaton (and for that matter, any CA) is described in the paper by Wiener & Rosenbleuth (1946). Greenberg *et al.* (1978*a*, *b*) classified all initial states that could lead to persistent behavior for excitable CA in which there are k_E excited states and k_R refractory states. Typical patterns seen in this type of model are shown in Fig. 1 and consist of square-rotating spiral waves. Multi-armed spirals, spiral pairs (Madore & Freeman, 1983), and three-dimensional waves such as twisted scrolls have also been noted in these simple models (Winfree *et al.*, 1985).

Numerous authors have explored different and increasingly complex rules in an effort to get quantitative agreement between the simulations and the experimental or more realistic numerical phenomena. Kaplan *et al.* (1988) study the dynamics of cardiac conduction in spatially *inhomogeneous* media with an excitable CA model. Fisch *et al.* (1990) characterize the behavior of numerous variants in which more than one excited neighbor is necessary or larger neighborhoods are considered. They have made available a CA simulator for personal computers. Gerhardt *et al.* (1990*a*, *b*, *c*) and Markus & Hess (1990) create excitable rules with quite different techniques that allow them to obtain quantitatively correct dispersion relations and spiral curvatures. The idea in Gerhardt is to let each cell consist of two components, corresponding to an "activator" and an "inhibitor" in a chemical reaction. By introducing many states and allowing spatial averaging over more than one cell distance away, they produce convincingly realistic pictures very rapidly on a small computer.

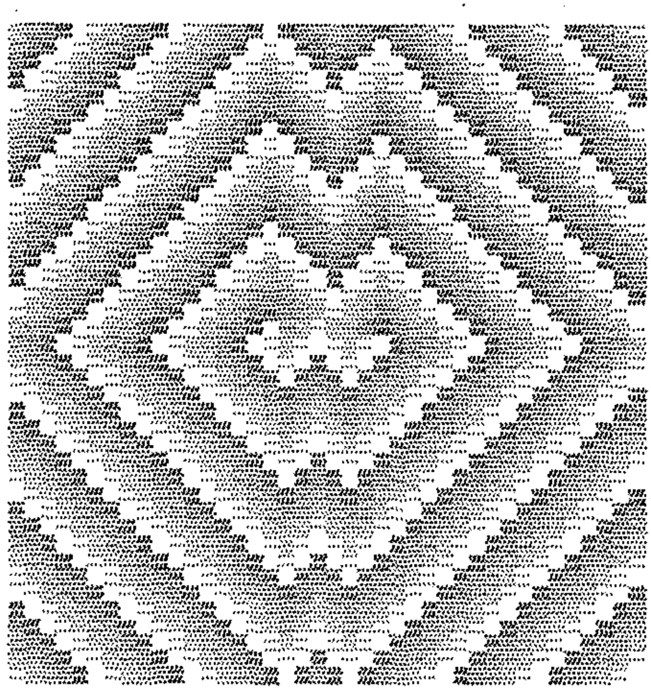

FIG. 1. "Spiral" wave pair in an excitable automata. There are six states, 0, 1, 2, 3, 4, 5. If any cell is in state 0 and at least one of its four neighbors is in state 1, it becomes state 1 at the next time step. If it has a non-zero state then it advances by one at the next time step until it is at state 5 where it returns to state 0. If at state 0 and no neighbors are in state 1, it remains at state 0. White corresponds to state 0 and dark grey to state 5.

Tyson and colleagues have devised increasingly more realistic models based on better discrete approximations to the Laplacian (Weimar *et al.*, 1991*a*, *b*). Markus & Hess (1990) obtain similarly curved spirals without resorting to such complex rules by allowing *long distance interactions* on a *random* spatial grid. They also simulate twisted scroll rings in three-dimensions.

While the rules used by these authors vary greatly, the mechanism for formation of spirals remains transparently similar; a recovery period, excitation of neighbors, and a threshold lead to spiral wave formation. These recent models have not been analyzed; indeed even the simplest rules which require, say, at least two excited cells to cause excitation have defied rigorous analysis.

2.2. DEVELOPMENTAL BIOLOGY

CA models have found use in some aspects of developmental biology. Young (1984) derives a simple model which uses the concept of lateral inhibition and threshold to create spatial two-dimensional patterns mimicking animal coat markings. In his rule, cells are in one of two states; the new state is found by spatially averaging over a circular neighborhood and applying a threshold function:

$$C_{i,j} = H\left(\sum_{(i',j')\in N} \mathbf{w}(i-i', j-j')C_{i',j'}\right),$$

where $\mathbf{w}$ is a matrix of weights or "mask" in the language of Tyson, N is a circular neighborhood, and $H(u)$ is the Heaviside function which is 1 for $u>0$ and 0 for $u<0$. A variety of coat markings are possible by varying the weights, the threshold, and the size of the neighborhood. In Fig. 2, we show the steady-state behavior for Young's model for two different weight functions. (See legends for details.) Spots and stripes occur as the "inhibition" is varied.

Swindale (1980) applies a similar rule to produce patterns of occular dominance in the visual cortex. Cocho *et al.* (1987*a*, *b*) use simple one-dimensional automata and transition rules to model the coat markings of fish, reptiles, and mammals. Models that allow for cell movement and some random factors have been proposed to mimic cell rearrangement and sorting. Bodenstein (1986) incorporates cell division and displacement to show how mixtures of two cell types can separate into distinct layers. Goel & Thompson (1988) also use automata models for cell sorting. A volume edited by Mostow (1975) contains numerous other models for cell rearrangement based on CA. Smith *et al.* (1984) derive a complicated set of CA rules to model the formation of microtubule arrays on the cell membrane. Hammeroff and coworkers have derived models of similar phenomena (Hammeroff *et al.*, 1986; Rasmussen *et al.*, 1990). Nijhout *et al.* (1986) propose a model for differentiation and mitosis which uses simple rules incorporation cell division, displacement, morphogens, differentiation, and mutations. By selecting different mutations, they derive a phylogenetic tree for abstract organisms. Dawkins [see the volume edited by Langton (1989)] has developed a similar simulation in which the software user selects organisms from a series of mutations at each step.

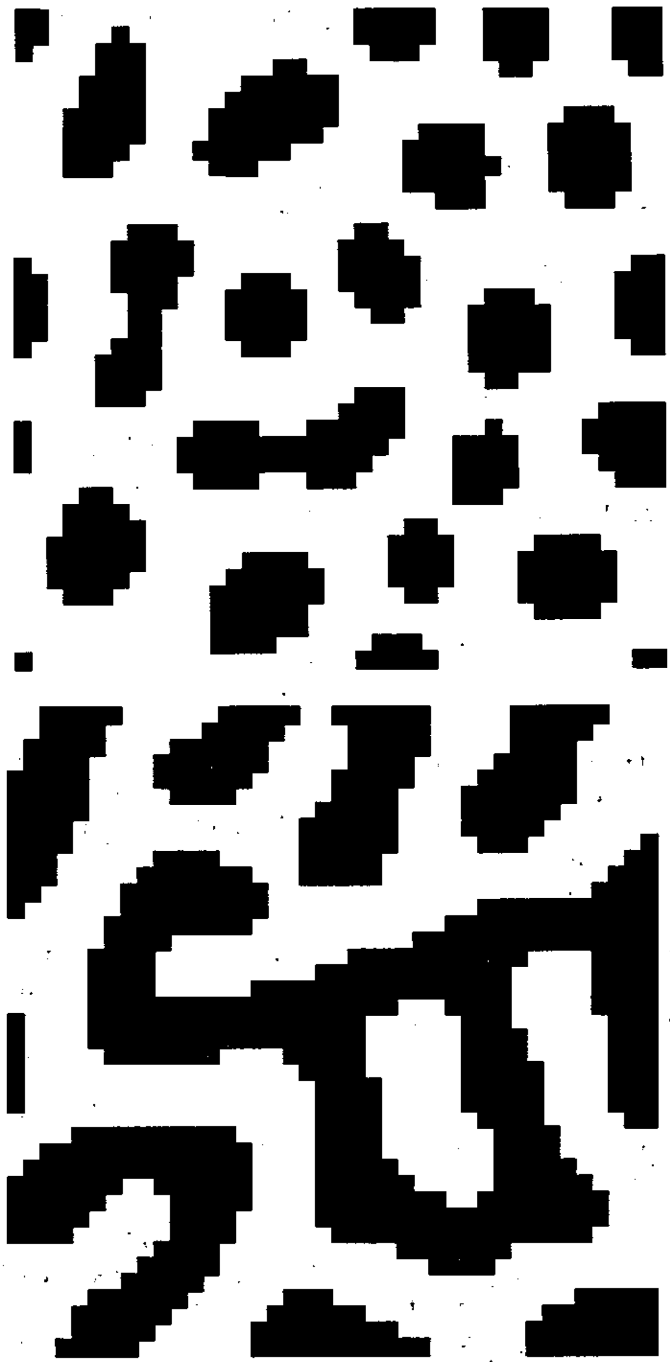

FIG. 2. Steady solutions to the Young model. White represents state 0 and black, state 1. The weights have a value of w_e for $(i-i')^2+(j-j')^2 \equiv R \leq r_e$ and w_i for $r_e < R \leq r_i$. For $R > r_i$, there are no interactions. In this figure, $r_e = 5$, $r_i = 36$, and $w_e = 1$. (a) $w_i = -0{\cdot}34$; (b) $w_i = -0{\cdot}24$.

2.3. ECOLOGY AND POPULATION BIOLOGY

There are a number of recent examples of models for predator–prey and ecology that use CA. WATOR is a family of ecological simulations involving sharks and fishes moving about on toroidal grid. The rules vary greatly (there is a newsletter available describing various situations—see Dewdney, 1988) but the model is basically a spatially distributed predator–prey system. The implementation of the model puts it under the category of a particle system. A typical WATOR simulation includes fish and sharks which randomly move around a grid. Sharks will starve after a certain number of generations, T_S, unless they find fish and reproduce after T_R generations. Fish reproduce after T_F generations and are destroyed when they encounter sharks. The behavior of this simple automaton is like that of the Lotka–Volterra predator–prey model.

Another particle system has recently been developed for the plant ecology in the Jasper Ridge Biological Preserve (Moloney *et al.*, 1991). There are two or more species of plants that produce seeds with random dispersal and random probabilities of germinating. Interspecific competition is allowed. The results of these simulations seem to explain some of the small and large scale patchiness in real ecologies.

Camazine (1991) describes a particle system or lattice gas automata for the formation of banded rings in honey bee combs. The model allows for random egg laying in empty cells that are close enough to other brood. Honey and pollen are randomly placed in cells and removed randomly at a rate proportional to the number of neighboring brood cells. These simple rules are sufficient to produce a very close approximation to the experimentally found patterns.

By simplifying a discrete time host–parisitoid model and placing the resultant system on a grid, Hassell *et al.* (1991) have been able to study spatial effects in these models. The form of the model is deterministic and is somewhat reminiscent of the excitable CA above. There are nine states, $A, B, \ldots, I$ and each state goes to the next state ($I \rightarrow A$) with two exceptions. State A goes to B only if there is one B neighbor. B represents a mature host colony. State D goes to state E only if one of the four neighbors is in state F which is the mature parasitoid. The automaton compares favorably with continuous state simulations of a spatial model. Figure 3 depicts output for this automata at a particular time; white is the absence of organisms, light stippling is host, and darker stippling represents parasitoids. The basic pattern slowly changes but stays qualitatively like that shown in the figure.

2.4. OTHER MODELS

The complexity of the nervous system and the difficulties with realistic models have led to some applications of CA to neural networks. Hoffman (1987) suggests a simple CA model for cortical electrical activity based on excitatory and inhibitory cells with simple dynamics. Modifications of the Hopfield model (Hopfield, 1982) in which the updating of the "neurons" is parallel rather than asynchronous leads to a CA. Indeed, let S_i^t denote the state of the i-th neuron at time t, then, the parallel

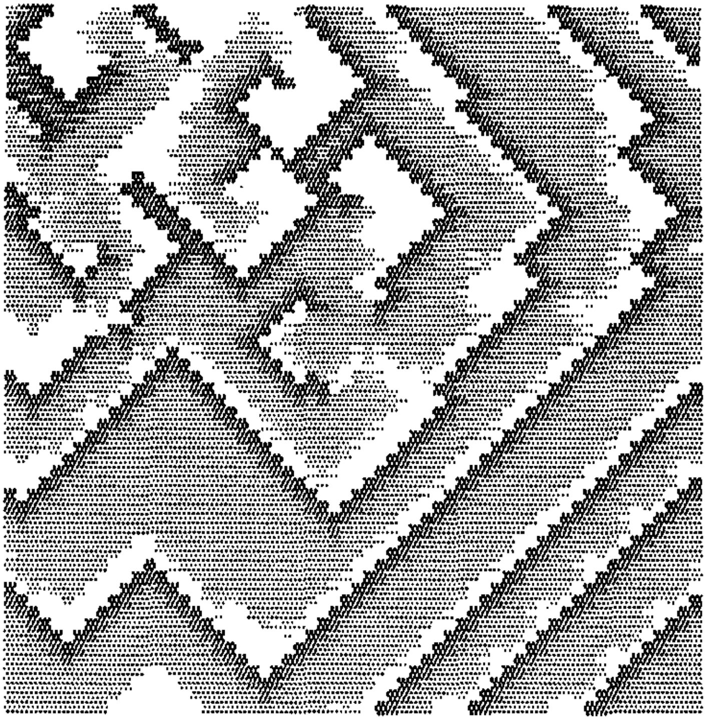

FIG. 3. Host–parasitoid automata. White is state 0 and dark grey is state 8.

version of the Hopfield model is:

$$S_i^{t+1} = H\left(\sum_j \mathbf{w}_{ij} S_j^t - \theta\right)$$

where $\mathbf{w}_{ij}$ is a weight matrix, H is the Heaviside function, and θ is a threshold. This is a two-state automata; the topology (i.e. line, plane, etc) of the network is determined by the weight matrix. Note that Young's model described above is a special instance of the "parallel Hopfield" model. An excellent example of a realistic CA model is the approach taken by Pytte *et al.* (1991) where they derive a simplified model of the hippocampal slice. The behavior of the simple model is qualitatively (*and quantitatively*) similar to that of a much more complex model that involves solving thousands of non-linear differential equations.

Other examples of CA applied to biology include models for immunology (Dayan *et al.*, 1988; Sieburgh *et al.*, 1990; DeBoer *et al.*, 1991), tumor growth (Duchting & Vogelssaenger, 1983; Chowdhury *et al.*, 1991), bacterial aggregation (Stevens, 1991), angiogenesis (Stokes, 1989) and "artificial life". The latter bears some additional mention; by artificial life (hereafter AL), we mean "the study of man-made systems that exhibit behaviors characteristic of living systems" (Langton, 1989). AL models are similar to CA in that they involve the dynamics of discrete objects. However, AL are generally more complex and often allow evolution to take place. For example, one might study the evolution of some simple trait such as clutch size to see which is more favorable. The recent volume edited by Langton describes some of these simulations. Related automata as well as other "artificial life forms" can be found in the book edited by Meyer & Wilson (1991). Kauffman (1984, 1990) has contributed a large body of work to automata as applied to evolutionary biology and complexity. A recent volume of *Physica D* (Forrest, 1990) contains related articles that are relevant to biological complexity.

3. Deterministic Automata

In this section, we describe a class of CA with completely determined rules; that is, once the initial state is known, all subsequent states are found by iterating and updating synchronously. In these types of automata, one considers the state of each position in an array of stationary cells rather than "following" the changing position of a single cell as in the next two sections. For this reason, we call these "Eulerian" automata, in analogy to fluid mechanics. This type of model is, in a sense, a limiting case of some partial-differential equation or integro-differential equation. Indeed, it is often desirable to make this analogy explicit in order to produce a realistic automata. [For example, Gerhardt *et al.* (1990*c*) use this method to create more realistic "models" for the Belousov–Zhabotinskii reaction.]

A general deterministic automata can be described in the following manner. The "world" consists of a discrete lattice of points, usually two-dimensional. Each lattice point is called a cell and takes on a finite number of states, say, $0, 1, \ldots, N$. The simplest automata have only two states. We let $C_t(i)$ denote the state of the cell at position i at discrete time t. To obtain the value of the i-th cell at the next time step, $t+1$, a rule is given which depends on the previous values of the cell and some (perhaps all) of the other cells:

$$C_{t+1}(i) = F(C_s(i), C_s(j)) \tag{1}$$

where $C_s(j)$ represents states of other cells in the lattice denoted by the index j at earlier times $s<t$. Typically, the dependence is on some small neighborhood of the cell. Suppose that there are N states per cell, m neighbors, and τ earlier time steps needed. Then the total number of possible rules is:

$$T_{\text{rules}} = N^{N^{(m+1)\tau}}$$

Often the rules are isotropic so that the dependence is on the states of the m neighbors but the neighbors are interchangeable. In this case the (N^m) component above is replaced by $(N^m/m!)$.

In a CA, cells often influence and are influenced by "nearest neighbors". However, a neighborhood in two-dimensions can be defined in several different ways. Each cell in a two-dimensional square lattice has eight nearest neighbors conveniently addressed as points on the compass. The four neighbors sharing a common face are: *N*, *E*, *S* and *W*. Those that can be reached diagonally are: *NE*, *SE*, *NW*, and *SW*. In a hexagonal lattice there are six neighbors. A finite, deterministic CA must eventually repeat since only finitely many states are possible on a finite grid. A simple calculation shows that for a total of M cells in the lattice, the total number of possible states is:

$$P_{\max}=M^{\tau N}.$$

Thus, $P_{\max}$ is the maximal period of the automaton. Periods of this length correspond to completely "stochastic" behavior. We define an automaton to be "periodic" if it repeats after $T<P_{\max}$ time steps. Realistically speaking, T is usually considerably smaller than the maximum.

The abstract properties of general deterministic CA have been the object of much study. The two volumes (Farmer *et al.*, 1984; Gutwitz, 1990) contain numerous theoretical and applied articles on the subject. Rather than focus on general aspects of CA, we will describe some techniques for deriving models from partial and integral equations. There are two main methods for derivation. The simplest is to abstract the observed phenomena into a few simple rules ignoring any explicit analogy to a fully defined mathematical model. The other approach is to directly discretize the mathematical model and obtain an automata. The former approach is used by Young (1984) and Hassel *et al.* (1991), while the latter has been exploited by Gerhardt *et al.* (1990*a*, *b*, *c*).

3.1. HEURISTIC CELLULAR AUTOMATA

The best known heuristic automata are the multi-state excitable media described in section 2. Conway's "LIFE" (Dewdney, 1988), which has little biological meaning other than a metaphor, is another example. ("LIFE" is a two-state automata on a two-dimensional grid with eight neighbors. If the cell is on and the sum of the neighbors is 2 or 3, the cell remains on. If the cell is off and the sum is 4, then it is turned on. Any other situations turn the cell off.)

3.1.1. *Age-structured predator prey model*

A somewhat naive, but instructive CA can be derived for an age-structured predator–prey interaction. We describe a single example although other rules can be used to create many more examples of arbitrary complexity. The present model is a deterministic analogue of the Monte Carlo simulation WATOR described in section 2. Consider an automaton with eight states: (0)-empty site, (1)-prey, (2)–(6)-predator stages (i–v), (7)-reproducing predator. The prey reproduce to fill nearest neighbor empty sites. Reproducing predators fill sites that have prey or that are empty. The progeny are then stage (i) predators and the parent "dies", leaving an empty site. Prey adjacent to predators disappear (are "eaten"). Predators require adjacent prey to consume in order to mature into the next stage. If prey is not available in an adjacent spot, they either become "hungry" or "die". In a 50×50 domain with periodic boundary conditions, randomly distributed prey and one or more initial predators, the automaton tends to form complex spatial patterns. The total predator and prey populations undergo complex oscillations with a period of roughly five time steps (see Fig. 4). Details of the completely deterministic rules are given in the figure legend. This model bears a resemblance to the model derived by Hassell *et al.* (1991). The total populations of sharks and fish oscillate fairly regularly much like a Lotka–Volterra model.

3.1.2. *Coupled oscillators*

CA are ideally suited for studying oscillatory media and exploring properties of these systems. The recent interest in systems of coupled non-linear neural oscillators has produced many results, but most of the analysis has dealt either with "all to all" coupling or with coupling of oscillators in one-dimensional chains. Two-dimensional oscillatory media have been infrequently studied and, due to analytic complexity, may be best initially explored by CA simulations. Here we propose a heuristic model for a locally coupled oscillatory medium.

The idea for this CA is based on the notion of a phase response curve. When an oscillator is stimulated, the result is a shift in phase compared to the unstimulated case. The curve of phase changes as a function of the phase of the stimulus is called the phase response curve (PRC). For an excitatory stimulus, the PRC is qualitatively like $-\beta \sin \phi$ where β is the magnitude of the stimulus and ϕ is the phase of the oscillator when the stimulus occurs.

Suppose each cell traverses m values, $0, 1, \ldots, m-1$ through which it cycles continuously. Thus, the period of the oscillator is m. (An excitable automata goes through a similar cycle, but stops at 0.) The interaction is defined as follows: If at least one of the neighboring cells is in state 0 (the firing state), then the new state is given by:

$$\text{new state} = \text{old state} + R[\text{old state}] + 1 \bmod m,$$

where R is the PRC of cell. Thus R is a list of m integers that approximates the "sinusoidal" shape of the PRC. This model, although simple, has many of the properties associated with non-linear oscillators with "pulsatile" coupling: phase-locking (the pair of oscillators fire once per cycle and have the same period), phase drift (the pair drift in and out of phase and behave almost as if uncoupled), subharmonic locking (one oscillator fires n times for each m of the second), and phase death (the coupling is so strong as to cause both to stop firing) are all possible for two such cells coupled together. Pacemakers and linear gradients are easy to simulate by allowing the individual cells to have different "periods", thus a comparison to continuous time and state-space models can be directly made. For example, "frequency plateaus", intervals of locked cells separated by complex quasi-periodic motion, are observed in a chain with a linear gradation in intrinsic frequency. A pacemaker region with a slightly higher frequency than the rest of the medium acts as a wave source and two such pacemakers can interact. If the frequency of the pacemaker is considerably higher than that of the remaining medium, the pacemaker cannot phase-lock the medium.

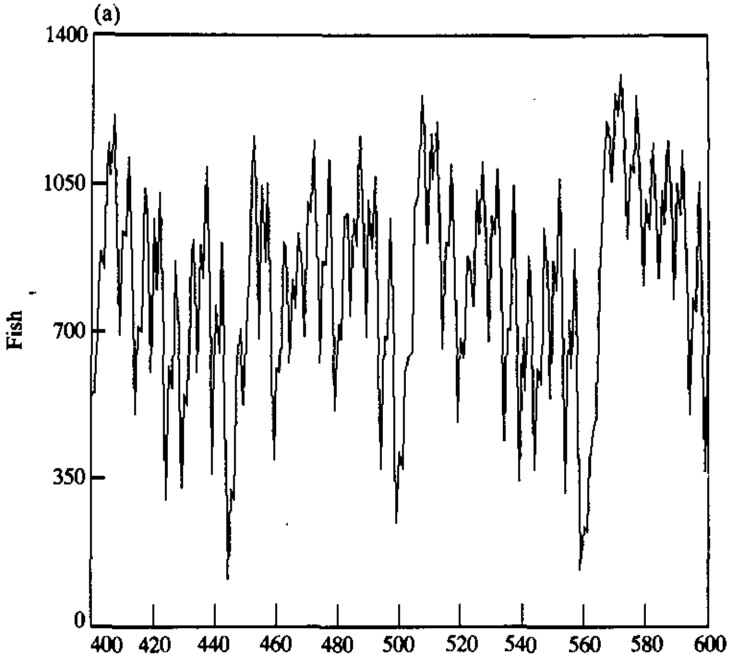
(a)
Fish
1400
1050
700
350
0
400 420 440 460 480 500 520 540 560 580 600

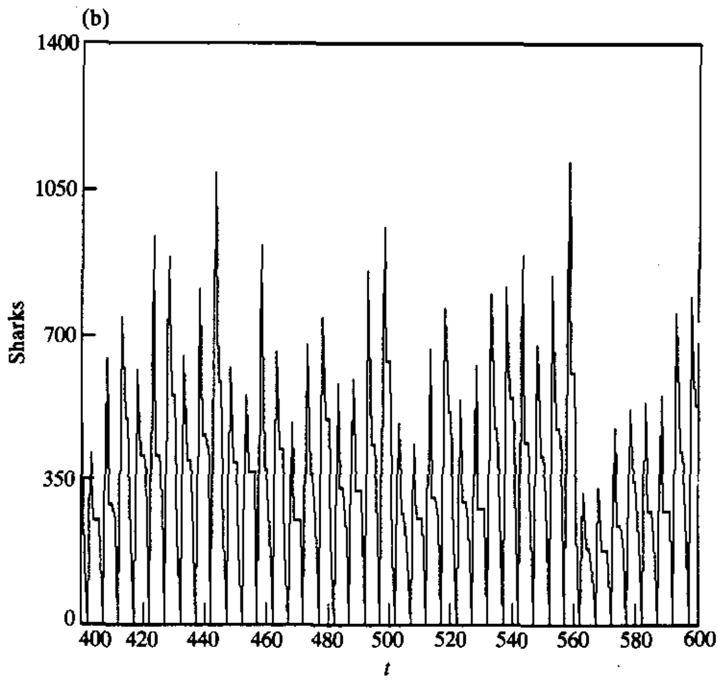
(b)
Sharks
1400
1050
700
350
0
400 420 440 460 480 500 520 540 560 580 600
t

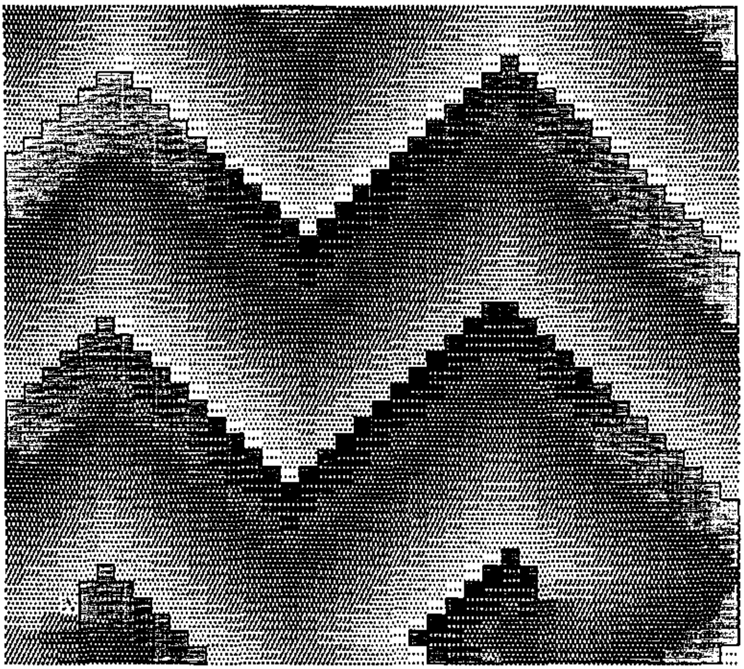

FIG. 5. Two-dimensional oscillatory automata with 16 states and nearest neighbor coupling showing development of a spiral wave. At each time step the automata advances by 1 modulo 16 unless at least one of its neighbors is in state 0, in which case it has an amount subtracted or added to it depending on its present state. The amount for states 0-15 is, respectively: (0, −1, −2, −2, −3, −2, −2, −1, 0, 1, 2, 2, 3, 2, 2, 1). White is state 0 and black is state 15.

If these cells are coupled in two-spatial dimensions through nearest neighbors we can ask whether synchrony (all cells oscillate with zero phase difference) is a necessity. We find that for small enough domain sizes, random initial conditions lead to synchrony. For larger domain sizes, persistent spatial patterns arise. Figure 5 shows such a spiral pattern. The "period" of the automata is best discerned by examining the "core" of the spiral (the spatial point about which it rotates). For the solution depicted, the period is 228 cycles in which time it "fires" 15 times. If this cell was uncoupled from the rest of the medium, 240 cycles would be required to fire 15 times. Thus the "spiral" wave has a higher frequency than the medium at rest and "takes over". The existence of spatial structures in this simple automata suggests that similar

FIG. 4. Temporal behavior of the automata PREDATOR. There are seven states in this model, 0 (empty), 1 (fish), 2 (shark 2), 3 (shark 3), 4 (shark 4), 5 (shark 5), 6 (shark 6), and 7 (mother). Empty sites are transformed into fish if any neighboring cells contain fish and into shark 2 states if any neighboring sites contain mothers. Fish states are transformed into shark 2 states if any neighboring sites contain mothers. Even shark states become empty if there are no neighboring fish sites otherwise they advance to the next state. Odd shark states advance to the next even state if there are no neighboring fish states. Otherwise they advance to the next even state. Mothers become shark 2 states at the next time step. (a) Fish versus time; (b) sharks versus time.

solutions may be found in more realistic models of coupled oscillators. We have recently confirmed this by proving the existence of rotating waves in two-dimensional discrete lattice of coupled continuous oscillators.

3.2. CELLULAR AUTOMATA FROM MORE COMPLEX MODELS

Since the numerical solution of the types of non-linear evolution equations that arise in biology involve so many unknown factors and are themselves simplifications of a system, it is often convenient to further simplify them in order to quickly ascertain their behavior. One approach is to reduce these models to finite automata which, because they work in integer arithmetic and use lookup tables, allow for a substantial increase in the speed of simulations. This approach is called "fixed point arithmetic" and is well known to programmers who use the language FORTH (which coincidentally is the language that Toffoli & Margolis use to drive their hardware CA simulator).

Suppose that one has derived a set of partial-differential equations for some deterministic phenomena. If the spatial domain of the model is continuous, then, we discretize the domain into finitely many regions. Boundary conditions are naturally applied to the discretization. If the time evolution of the model is discrete, then nothing needs to be done. Otherwise, one approximates the time-derivative by a simple discretization such as Euler's method. Generally, time and space discretization of a problem is obvious; the art and most difficult problems arise in attempting to discretize the state space. In most biological models, reality constraints force the dependent variables to lie in some finite bounds. (For example, in neurobiology, there will be a maximal neural firing rate, in ecology, a carrying capacity, etc.) If one can bound the dependent variables, then the final step is to break each state variable into a fixed number of parts and scale all variables so that the states are integers. Using these discretizations, rule tables are made and the CA is ready to be simulated. In the following, we will apply these techniques to several continuous problems.

3.2.1. *A reaction–diffusion system*

Consider the two variable reaction–diffusion equations in the plane:

$$\begin{aligned} u_t &= f(u, v) + d_1 \Delta^2 u \\ v_t &= g(u, v) + d_2 \Delta^2 v. \end{aligned} \tag{2}$$

Here, u, v might represent chemical concentrations, populations of animals, or electrical activity of cells and f, g represent the interactions between these two components. The spatial interaction is via diffusion. The first step is to discretize this system in time and space which leads to:

$$\begin{aligned} u_{\text{new}} &= u(1-\lambda_1) + \lambda_1 (u_N + u_E + u_S + u_W)/4 + \Delta t f(u, v) \equiv F(u, v, \bar{u}), \\ u_{\text{new}} &= v(1-\lambda_2) + \lambda_2 (v_N + v_E + v_S + v_W)/4 + \Delta t g(u, v) \equiv G(u, v, \bar{v}) \end{aligned} \tag{3}$$

where $\lambda_j = 4d_j\Delta t/(\Delta x)^2$ and $(\bar{u}, \bar{v})$ are the mean values of the four neighbors of (u, v). Δt is the minimum time step of interest (e.g. it could be msec for neurons or months for populations of animals) and $\Delta x = \Delta y$ are the minimum spatial scales of interest. For numerical procedures, it is generally assumed that $\Delta t = O(\Delta x^2)$ but this is unimportant for deriving CA. One can use a more accurate approximation of the Laplacian operator than the simple average of four neighbors but for the present discussion, this is unnecessary. Suppose we have chosen the functions f, g so that we can bound the variables u, v to lie in a finite interval. Then, we rescale (3) so that the values of u and v are always between 0 and 1. This in turn implies that the rescaled functions F, G lie between 0 and 1. The interval [0, 1] is broken into $N+1$ pieces and (3) is used to build a state transition function for the new values $(u_{\text{new}}, v_{\text{new}})$ on this integer grid. Thus, a correspondence is made between the values of u, v and each of the integers, $0, \ldots, N$, with $0 \to 0{\cdot}0$ and $N \to 1{\cdot}0$. This enables us to produce two "functions" $\mathscr{F}(i, j, k)$ and $\mathscr{G}(i, j, k)$ which are defined to be the closest point on the grid to $F(i/N, j/N, k/N)$ and $G(i/N, j/N, k/N)$. More generally, one uses a different value of N for each variable. Gerhardt *et al.* (1990*a*, *b*, *c*) perform essentially this same procedure in order to produce a reaction–diffusion model that accurately mimics the Belousov–Zhabotinskii kinetics. The recovery variable in their model has many states, while the excitation variable has only two states.

We can easily apply the above method to produce an automata which shows spatial pattern formation, oscillations, and complex, slowly varying spatial patterns similar to those observed in some reaction–diffusion models. There are many activator–inhibitor systems from which to choose; by using a caricature of sigmoidal

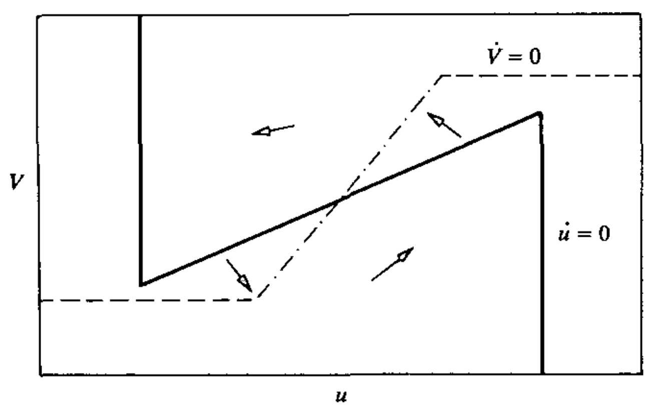

FIG. 6. The "phase-plane" for eqn (4). The kinetics for this figure are $f(u, v) = \beta(-u + 16H(12u - 16v + 32))$, $g(u, v) = \alpha(-v + [2(u-4)]_0^{15})$. Here $H(u)$ is the Heaviside step function with the stipulation that $H(0) = 1/2$ and

$$[x]_a^b = \begin{cases} b & \text{if } x \geq b \\ a & \text{if } x \leq a \\ x & \text{otherwise.} \end{cases}$$

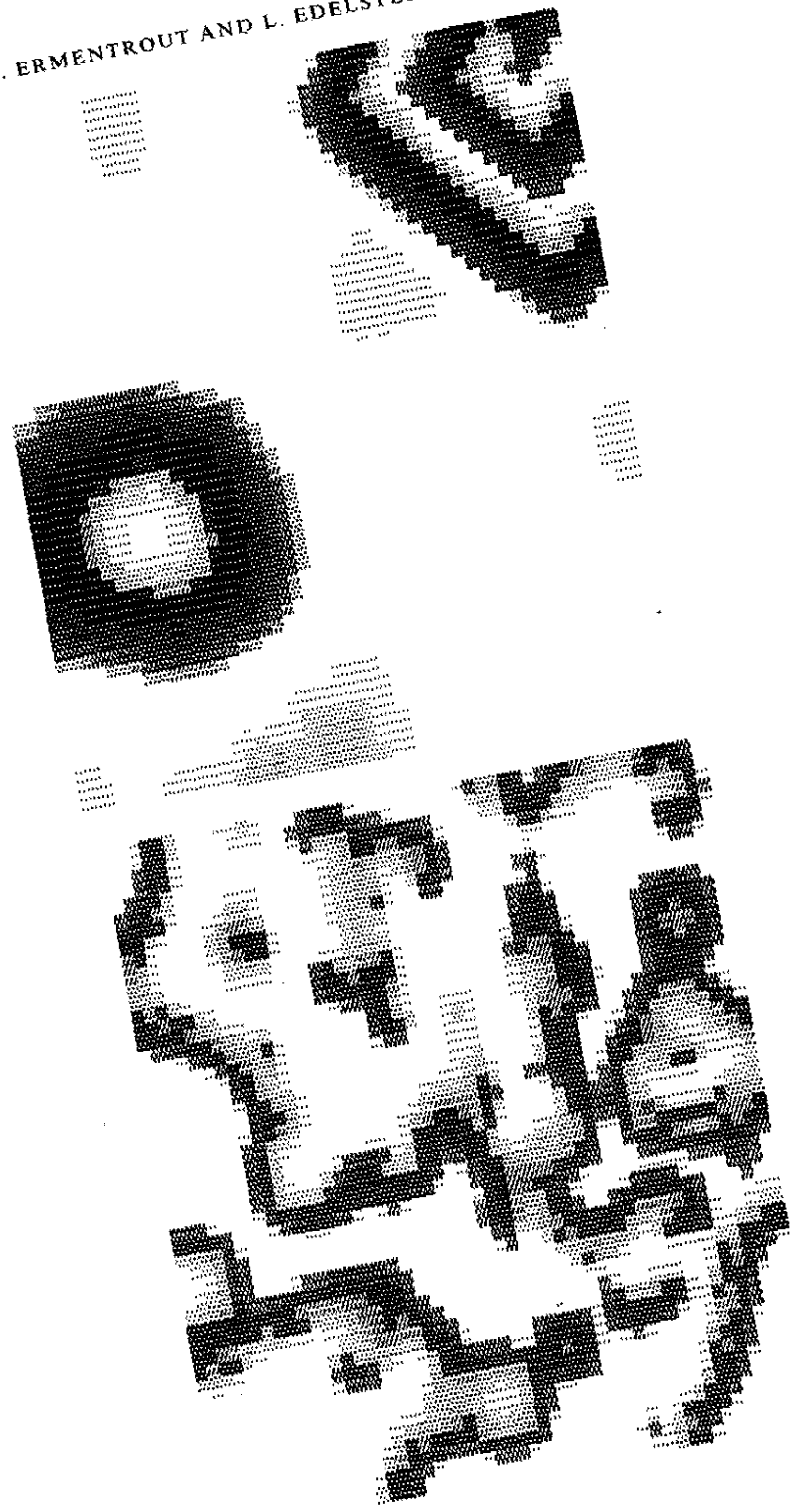

interactions with decay and autocatalytic self-excitation, one can produce a simple two-variable model with nullclines as shown in Fig. 6. By "sigmoidal" inter-reactions, we mean that the effects of the activator are initially small followed by a rapid increase and then a saturation. This type of model occurs frequently in the activator-inhibitor literature and is meant to caricature a kinetic interaction of the form:

$$\frac{K_1 u^2}{K_2 + u^2}$$

where K_1, K_2 are constants and u is the concentration of some substrate.

The phase-plane in Fig. 6 is typical in biological settings [see e.g. figs 5.6–5.8, 6.4 in Murray (1989)]. This choice of kinetics constrains both u and v to lie in the interval [0, 15). We let each of the two variables have 16 possible states, thus there are a total of 256 states. The parameters in the automata are the rate constants $\Delta t\ \alpha$ and $\Delta t\ \beta$, the threshold, θ, and the diffusion parameters λ_1 and λ_2. The "rate constants" are not to be interpreted too literally here, but rather as a means of characterizing the relative rates of the activator and inhibitor as compared to the relative diffusivity. That is, these parameters essentially determine the relative importance of the local kinetics compared to the effects of neighbors on the transition to new states. By varying these rate constants we can make the activator faster or slower than the inhibitor; similarly, by varying the diffusion parameters λ_j we can create lateral inhibition or activation. In Fig. 7, we show some of the dynamic behavior of this automaton that mimics a non-linear activator inhibitor system.

Accuracy of this model with respect to the continuum equation can be improved by using more accurate discretizations of the Laplacian as Tyson and colleagues have done (Weimar *et al.*, 1991*a*, *b*).

3.2.2. *A model for shell patterns*

The CA in section 3.2.1 uses nearest neighbor coupling. Integral equations in space can also be discretized to produce CA with longer range interactions. A neural model for molluscan shell patterns incorporating long-range interactions is proposed in Ermentrout *et al.* (1985). They present a discrete time, continuous space system of neural equations that is easily converted to a CA. Let x_n^j denote the pigmentation of position j and row n on the surface of the shell. x is either 0 or 1 depending on pigmentation. If the neural activation and inhibition (obtained by sensing the pigment previously deposited) differ by some amount, new pigmentation occurs. Thus

FIG. 7. Two examples of dynamics for the activator-inhibitor model described by eqns (3–4). The parameters are (λ_1, λ_2, $\alpha\Delta t$, $\beta\Delta t$, θ). Top figure: target and spiral in the same medium. Both patterns expand outward periodically in time [50, 10, 50, 20, 0). Bottom figure: slowly moving striped pattern [40, 70, 40, 30, 3). Activator states are shown with state 0 colored white and state 15 black. [Note: stationary patterns showing effect of lateral inhibition occur for parameters (30, 60, 55, 16, 7).]

they arrive at the following equations:

$$\begin{aligned} x_{n+1}^j &= H(A_n^j - I_n^j - \theta) \\ A_n^j &= F_a\left(\sum_{k=0}^{\tau-1} \sum_{l=-b}^{b} w_{kl}^a x_{n-k}^{j+l}\right) \\ I_n^j &= F_i\left(\sum_{k=0}^{\tau-1} \sum_{l=-b}^{b} w_{kl}^i x_{n-k}^{j+l}\right) \end{aligned} \tag{4}$$

where A_n^j is the activation, I_n^j is the inhibition, w_{kl}^σ are positive weighting functions (usually piecewise constant), H is the Heaviside function, θ is a threshold, and F_σ are saturating non-linearities. The discussion of this model can be found in Murray's book (Murray, 1989) or in Ermentrout *et al.* (1985). Each x_n^j is either 0 or 1 and the activation, A_n^j and inhibition, I_n^j depend only on the weighted values of x_j^n. Thus, we can rewrite (4) as:

$$x_{n+1}^j = \mathscr{F}(x_n^{j-b}, \ldots, x_n^{j+b}, \ldots, x_{n-\tau+1}^{j-b}, \ldots, x_{n-\tau+1}^{j+b}).$$

This is a two-state automata. There is an astonishing variety to the patterns that this automata can make. In particular, most of the patterns in Ermentrout *et al.* (1985) can be readily simulated. For purposes of comparison, we note that the "totalistic" rules of Wolfram (1984*a*, *b*) are of the same form as (4) provided that we choose the weights w_{jk}^m appropriately and $\tau = 1$. Molluscan patterns are also modeled by CA in Gunji (1990) and Vincent (1986).

3.2.3. *An immunological model*

So far all of the examples in this section have utilized local rules in that interactions depend only on the state of the cell and some of its *nearest* neighbors. Recently, DeBoer *et al.* (1991) describe a continuous state "cellular automaton" for shape-space simulations of the immune system. This model is a simplification of a continuous time integral equation in space. The interactions are not with neighboring sites, but rather, with the complementary sites. That is, if the system is on an $N \times N$ grid, then the interactions of cell (i, j) depend on $(i', j') \equiv (N - i, N - j)$. From their model, we obtain the simple 16 state model for the number of "B-cells", b_{ij} at point (i, j) in state space:

$$b_{ij}^{t+1} = \begin{cases} \min(b_{ij}^t + 1, 15) & \text{if } \theta_1 \le h_{ij}^t \le \theta_2 \\ \max(b_{ij}^t - 1, 0) & \text{otherwise} \end{cases}$$

where,

$$h_{ij}^t = w_0 b_{i'j'}^t + w_1(N' + S' + E' + W') + w_2(NE' + NW' + SE' + SW').$$

Here, N' means the northern neighbor of $b_{i'j'}^t$ at time t. The five parameters w_0, w_1, w_2, θ_1, and θ_2 are non-negative integers. The effect of taking the maximum and minimum values is to apply a piecewise linear approximation to a saturating non-linearity. In Fig. 8, we show the result of a simulation of this automata. The shading at the (i,j)-th node indicates the number of cells with the "shape" (i,j); white is the lowest and black is the highest. If instead of the complementary rule, we just allow local interactions, the resultant pattern consists of lines of cells that are at 0 or 15; no complex spatial patterns occur. The idea of this model is to mimic the interactions of B cells in a simple two-dimensional shape space. Here, the two dimensions of the model do not correspond to real space but rather to some abstract properties (e.g. the shape of an antibody) characterizing the B cells. The variable h characterizes the total stimulation of each population of B cells which comes from the complementary "shape", $(N-i, N-j)$. For details on the biological justification of this model as well as some analyses of the continuous case, consult (DeBoer *et al.*, 1991).

There are many other examples of realistic models that can be converted to automata. A model that is too simplistic admits no biological interpretation, whereas an overly complex model does not permit exploration of a wide range of different parameters in large spatial domains. Thus, a balance must be struck between the conflicting desires of realism and biological interpretability on one hand, and the basic aim of keeping the simulations simple to avoid lengthy computations.

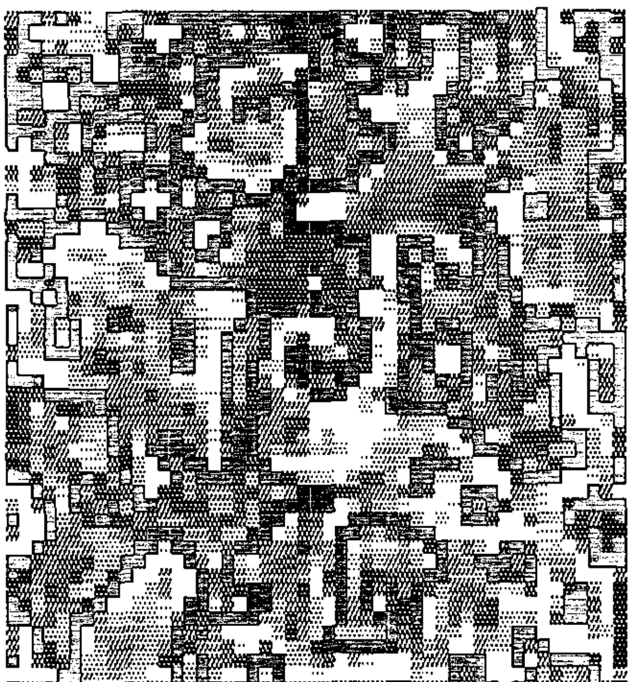

FIG. 8. Slowly varying spatial pattern for the "immune" model defined by eqn (3.8). State 0 is white and state 1 black.

4. Biological Lattice Gases

In the previous section, we examined examples of automata in which there is some quantity at every point in the grid and the evolution of this quantity was determined by the present state and previous states. Here, instead, we follow "particles" which stand for cells, organisms, or molecules as they move about the empty grid points. The particles move and bind to the medium, but binding is assumed to be reversible. (Irreversible binding is the subject of the growth models of the next section.) We present three examples of this sort ranging from the subcellular to the organismic level. The models exhibit collective organization that can often be modeled by a simpler continuous dynamical system, albeit at the risk of losing spatial information. Indeed, in Edelstein-Keshet & Ermentrout (1990*b*), we apply this spatial homogenization to determine the density of cells at which parallel arrays are formed in fibroblast aggregates.

The basic idea of what we call a "lattice gas" is that particles move in a medium (whether randomly or deterministically) over a discrete lattice and undergo state changes when they collide. The primary interest is the steady-state behavior of the system, or more specifically in the case of biological models, in the steady spatial pattern. Examples of this type have been applied to fluid dynamics (Frisch *et al.*, 1986; Doolen & Montgomery, 1987; Chopard & Droz, 1988), spin glasses (Farmer *et al.*, 1984), billiard ball computations (Farmer *et al.*, 1984; Vichniac, 1984), and ferro-magnetism (Wolfram, 1986). Note that, unlike models of section 3, probabilities are involved in these models, and thus, the initial configuration does not uniquely specify the dynamics. This is an advantage since different initial states are unlikely to lead to different final configurations. Thus, only the parameters and not the initial data must be varied. A well-known tool also based on probabilistic events is the Monte Carlo simulation, which has a long history in numerical computation of PDEs. While Monte Carlo simulations are closely related to our simple models, they differ in permitting a continuum of values where, in our models, the number of permissible states is limited. Some previously described examples of lattice gas models are the WATOR simulation, Camazine's model for honey combs, and the ecological model of Moloney *et al.* (1991).

It would be impossible to adequately survey all know lattice gas models in this brief space. We shall instead describe three examples that have arisen in our own research.

4.1. FIBROBLAST AGGREGATION

Experiments using cell cultures of fibroblasts show that as the density of the cultures increase, the cells begin to line up into "parallel arrays". In Edelstein-Keshet & Ermentrout (1990*a*, *b*) we describe a model for this phenomenon, derive continuous integro-differential equations, and obtain conditions for pattern formation as functions of the cell density, turning rate, and binding rates. Cells with initially random orientations are placed in a dish. The cells crawl and make occasional random turns. If a cell comes into contact with other cells or with groups of cells it attempts to align, provided the angle of contact is sufficiently small. As groups of aligned cells form, they recruit other cells into an array that has a definite direction. Cells in an array do not reorient. If the total number of cells is sufficiently large, eventually only a few arrays of cells of similar orientations are obtained. For a small number of cells, parallel arrays form only transiently.

In our automata, we consider N cells in an $m \times m$ array with periodic boundary conditions ($N < m^2$). With each cell C_j we associate an orientation as well as a state (bound or unbound). The cell's orientation determines its direction of motion for the next time step. There is a fixed probability P_0 of reorienting by one angular unit per time step. For example, if eight orientations are used to discretize angles, then the cell moves to the appropriate neighbor, turning by one unit with probability P_0. If, instead, 16 orientations are used, the movement direction depends on whether the time step is odd or even. (A cell that is oriented halfway between N and NE will make a north step followed by a northeast step at the next time step.)

At each time step, an unbound cell may reverse its direction of motion with probability P_R. If it comes into contact with another cell or group of cells, the probability of binding and aligning is P_A if the angle of contact is small enough. Otherwise, the approaching cell reverses direction and moves away. Bound cells do not move. The probability that a bound cell detaches from a group is P_D.

The simulation begins with all N cells unbound and assigned random orientations. Total numbers of cells in each orientation are tabulated and the simulation is followed until a steady state appears to be reached. Assuming "well mixing" (i.e. neglecting spatial structure) we show in (Edelstein-Keshet & Ermentrout, 1990*b*) that if the total number of cells is large enough (say, N^*) then parallel arrays will form. In Fig. 9, we depict a simulation involving $N < N^*$ cells. There are transients that last for a long time, but no orientation eventually wins out. Figure 10 shows the same simulation with $N > N^*$. Parallel arrays quickly form.

To give the reader some of the flavor for the mathematics that arises, we derive the continuum models for this automata. Let $n(\theta, t)$ denote the number of free cells in the array with orientation θ at time t. Let $b(\theta, t)$ be the number of bound cells. The probability of a collision between two free cells is $n(\theta, t)n(\theta', t)/V^2$ where V is the volume (or in the present case, the area) of the "dish". Similarly $n(\theta, t)b(\theta', t)/V^2$ is the collision rate of bound and free cells. From this we see the following must hold:

$$
\begin{aligned}
n(\theta, t+1) = n(\theta, t) - P_A n(\theta, t) \frac{1}{V} \sum_{\theta'} K(\theta - \theta')(n(\theta', t) \\
+ b(\theta', t)) + P_R(n(\theta + \pi, t) - n(\theta, t)) + P_D b(\theta, t) \\
+ P_O(n(\theta + \delta, t) + n(\theta - \delta, t) - 2n(\theta, t)) \qquad (5)
\end{aligned}
$$

for the unattached cells. The first term is the interaction between all other orientations that causes loss of free cells. The function K is 1 if the difference in the angles is small enough and 0 otherwise. The P_R term arises from the ability of cells to reverse

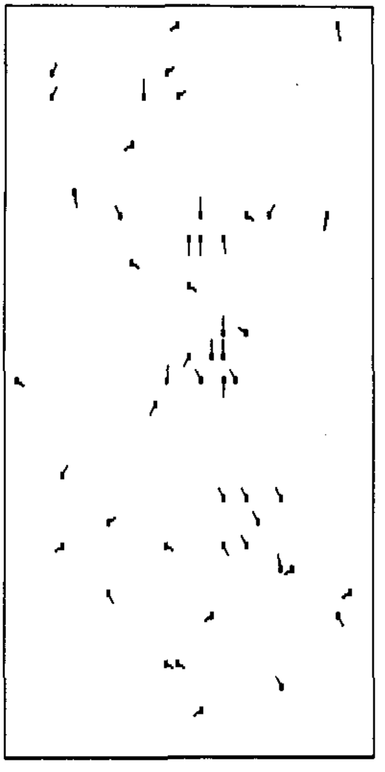

FIG. 9. Fibroblast automata for $N<N^*$ showing inability for one orientation to dominate. There are N "cells" in 16 different orientations that randomly move about the square with periodic boundary conditions. Each cell has a probability p_0 of reorienting. If two cells bump into each other and are not perpendicular in orientation, they align at one of the two orientations with probability p_a and become bound and immobilized. Similarly a single cell that runs into a bound cell will stick to the bound cell with probability p_s. Cells can fall out of the bound state with probability p_i. Spatial arrangement after over 10 000 iterations. The parameters are $N=50$, $p_a=0{\cdot}99$, $p_o=0{\cdot}05$, $p_i=0{\cdot}1$, $p_s=0{\cdot}99$.

direction, the P_D term is the rate of detachment from bound cells, and the P_O term arises from reorientation to the next close angle. For the bound cells, we have:

$$b(\theta, t+1)=b(\theta, t)+P_A(n(\theta, t)+b(\theta, t))\frac{1}{V}\sum_{\theta'} K(\theta-\theta')n(\theta', t)-P_D b(\theta, t). \quad (6)$$

In our analysis of these equations (with continuous time) it is shown that if the number of cells is sufficiently great (or equivalently, if the domain is small enough), then an instability of the homogeneous steady state arises and one orientation is selected. The continuum model proposed above does not incorporate spatial patterns which is why we use the CA model. The full spatial equations would be very complicated (see e.g. Edelstein-Keshet & Ermentrout, 1989).

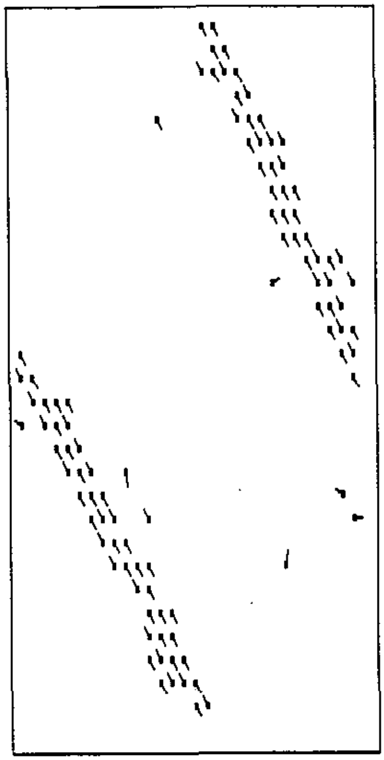

FIG. 10. Same as Fig. 9 but $N = 100$. This depicts the state after 6500 steps.

4.2. OCCULAR DOMINANCE COLUMNS

Occular dominance columns are regions in the visual cortex of the brain which receive neural signals from one of the two eyes. During development, different nerves with signals from each eye must grow towards and form contacts (synapses) with target tissue in the visual cortex. As a result, the region becomes organized into striking spots and stripes of left versus right eye dominated regions, i.e. occular dominance columns. (These can be visualized by radiolabeling experiments.) The problem of formation of these patterns of occular dominance has been a subject of numerous mathematical and experimental studies (Fraser, 1980; Swindale, 1980; Miller *et al.*, 1989; Fraser & Perkel, 1990). Many of these studies are based on the idea that the target tissue within the cortex is initially homogeneous and the formation of synapses somehow enhances the creation of more synapses of the same occularity. The mechanism for this affinity could be activity dependent (i.e. Hebbian) or it could depend on some chemical affinity (see e.g. Fraser & Perkel, 1990). Hebbian synapses strengthen if the pre- and post-synaptic activities are correlated. In the chemical affinity model, "like" axons attract each other through chemical markers.

We briefly describe such a model using biological lattice gases. Consider a lattice of unoccupied sites filled with freely diffusing particles of two types, say L and R.

The particles represent crawling neurites that emanate from the left and right eyes, respectively. The lattice represents the target tissue. At any given time there is a probability of binding to a free site, P_B as well as a probability of unbinding if already attached, P_U. It is clear that if the probabilities were fixed, no driving force for the emergence of pattern would exist, and no pattern would emerge. Thus, we assume that these probabilities depend on the number of neighbors that are of the same type as the given neurite, namely, we assume that the probability of binding, P_B is an increasing function and that the probability of unbinding P_U is a decreasing function of the number of like neighbors. We investigate whether such neighborhood effects suffice to induce spatial segregation.

If the probabilities are uniform, then initially random assortments of cells remain random and no segregation occurs. In contrast to this, Fig. 11 shows the results of a simulation when the binding rates are state dependent. The phenomenon of segregation is clear cut. We observe, further, that the average spacing of the segregated patches is not identical with the spatial length scale of an interaction but is rather much larger. The (analytic) determination of this spacing as a function of the probabilities is an open problem. (We have begun analysis of a deterministic model in one spatial dimension which may partially address this question.)

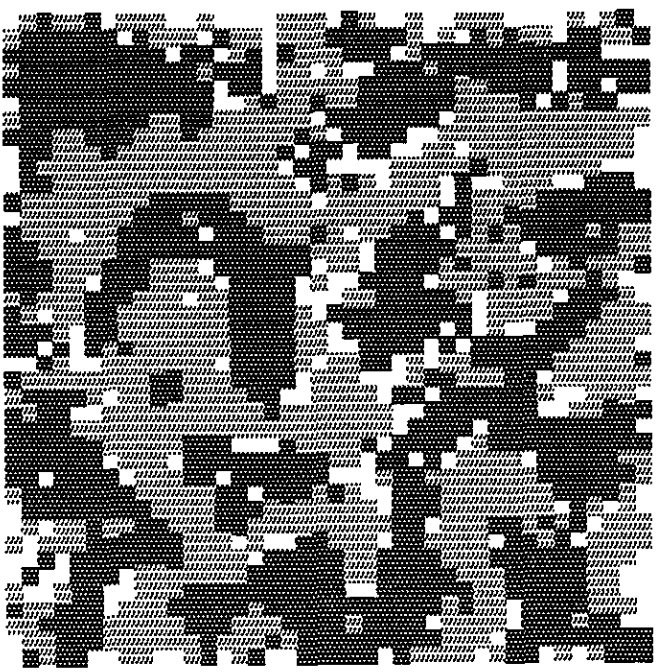

FIG. 11. DOMINANCE automata for modeling the formation of occular dominance columns. There are two types of "cells", dark and light and a two-dimensional array of grid points. A cell occupies a grid point with a probability dependent on the neighborhood of the grid point. The probabilities of binding increase as the number of neighbors that are of the light or dark type increase. This leads to a stripe-like pattern and definitive boundaries between cell types. In the absence of state-dependent probability, no pattern is formed.

Several variants of the preceding occular dominance automaton can be envisioned. First, clearly, a simulation of this sort need not be restricted to two cell types; rather one could generalize this to k different neurite types, possibly arriving at a model for orientation preference (see e.g. Miller *et al.*, 1989). Further, it is also possible to treat the transition rules in a quasi-deterministic fashion. A deterministic model that has much the same behavior as our original two-state system is described below.

Initially suppose that two states L and R are randomly distributed on an $m \times m$ grid. Let a neighborhood be defined as a central square together with it eight nearest neighbors. Let σ represent the sum of members of a neighborhood that are in state L. If $\sigma = 6, 7, 8$, or 9, in the next step the state of the central square becomes L. On the other hand, if $\sigma = 0, 1, 2$, or 3, the transition is to R. When $\sigma = 4, 5$ neither is a clear winner, so the "majority rule" is reversed: i.e. if $\sigma = 4$, the state changes to L but if $\sigma = 5$ it changes to R. Such switching is important in order to permit some "random" change to occur when a balance between types exists. This particular automata, called "ANNEAL" in Toffoli & Margolis (1988) is used as a model for annealing. The edges slowly are eroded away, but the stripe-like quality remains. In Fig. 12 we show a typical result of this simulation.

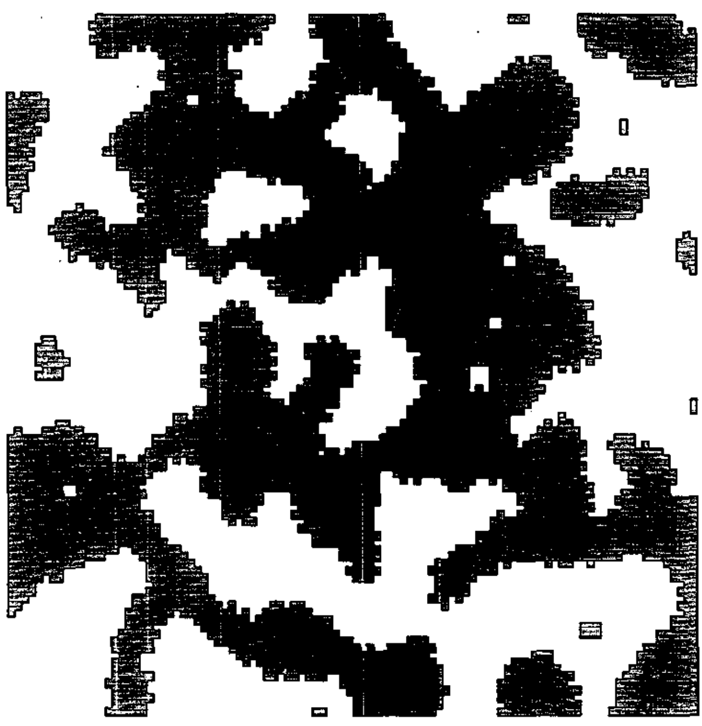

FIG. 12. Simple model based on the automata ANNEAL described in the text. Here, state 0 is white and state 1 is black.

4.3. SELF-ORGANIZATION OF ANT TRAILS.

Ants are known to communicate by a variety of means including chemical (pheromone) signals that they deposit along their trails. A pheromone trail deposited by a worker returning from a food find to the nest elicits recruitment of fellow workers to the find (Deneubourg *et al.*, 1989). Various types of foraging ants, and particularly army ants, continuously secrete pheromone even in the absence of food (Holldöbler & Wilson, 1990). Our interest is in the possible range of behavior that arises when individuals create (or reinforce pre-existing) trails while attempting to follow new trails that they cross. One expects limiting cases in which ants fail to find one another's trails and remain solitary, or in which a small subset of trails carry the majority of the traffic. A striking example of the latter which actually occurs in nature, is the "ant mill", a closed circular path in which ants (mostly army ants) follow each other meaninglessly to the point of starvation and death [see figs 12–16 in Holldöbler & Wilson (1990)].

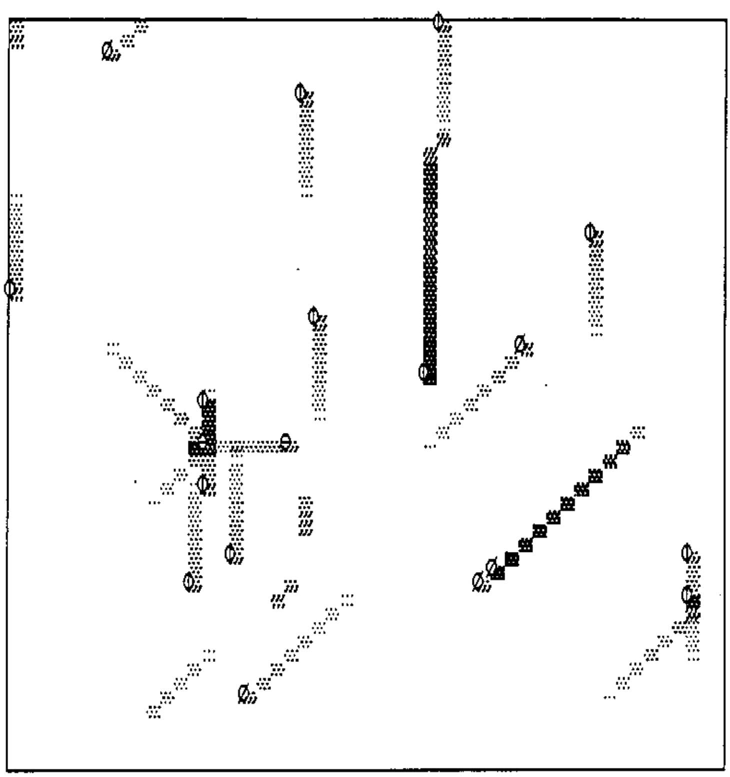

FIG. 13. Ant automata showing snapshots at three different times. There are 20 ants on a 50×50 grid. The parameters are $K_{max} = 30$, $K = 18$ when on the trail, $K = 8$ when off, $P_{on} = 0{\cdot}001$, and $P_{off} = 0{\cdot}01$. First figure: early part of simulation showing disordered movement ($T = 24$). Second figure: later two strong trails arise ($T = 1728$). Third figure: eventually a single trail dominates ($T = 4032$). This persists at least until $T = 12\,000$ when the simulation was stopped.

We now describe a very simple spatial model for trail following in ants which could possibly apply to other types of organisms. Consider an $m \times m$ grid with periodic (toroidal) boundary conditions as we have encountered in previous examples (i.e. a particle leaving from one edge, returns at the opposite edge). On this lattice, a population of N ants moves in random directions. Each ant secretes a pheromone trail which then evaporates at some rate. Other ants encountering this trail will possibly turn (by an acute angle) and follow the trail, also depositing pheromone along it. If the ant approaches the trail at a right angle, it crosses and ignores the trail. While following a pre-existing trail, the ant has a probability P_{on} of losing the trail by turning away from it. A solitary ant makes occasional random turns with probability P_{off}. Generally $P_{off} \gg P_{on}$.

An amount K of pheromone units is secreted by each ant every time step. K depends on whether or not the ant is on or off the trail; generally, more pheromone is secreted when the ant is on the trail. We assume that the maximal pheromone level at a lattice site cannot exceed K_{max}. (The level is artifically set to this maximum if it exceeds it at any location.) Pheromone "decays" at the rate of one unit per time step, so that a solitary trail disappears (from the rear) after K_{max} time steps. The

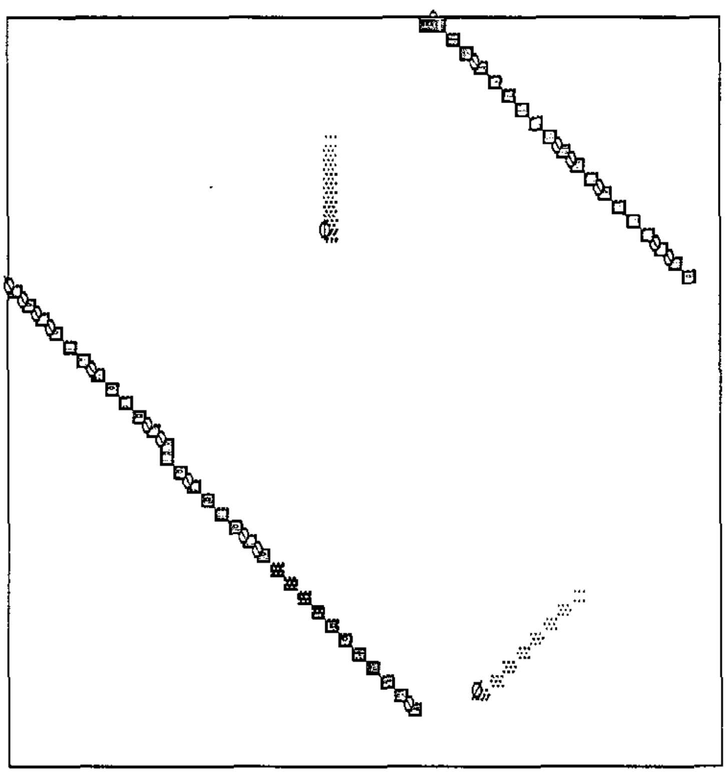

FIG. 13—continued.

domain size is assumed large relative to the diffusional range of the pheromone so that a simulated ant senses the trail only when crossing it directly.

The automaton requires seven parameters: the size of the grid, m, the number of ants, N, the maximum pheromone allowed on one site, K_{max}, the amount of pheromone deposited by an ant on the trail, K_{on}, the amount when off the trail, K_{off}, the probability of turning when not following a trail, P_{off}, and the probability of turning when on the trail, P_{on}.

In Fig. 13 we show snap shots of the ANT automaton simulation incorporating the above rules. In the earliest stages, ants move about in a disordered way, but in time, most are following some trail. In the last frame, all ants are on a single trail circling around the domain. For a larger number of ants, the behavior is somewhat different: several "trunk" trails evolve and the "ants" move between these, but a single dominant trail does not evolve (see Fig. 14).

We have recently derived continuum models for trail following that explain some of the phenomena in this discrete model. Roughly, we assume that there are many trails and that ants choose between them depending on a difference in pheromone concentration. This effect is "autocatalytic" since as ants cross from one trail to

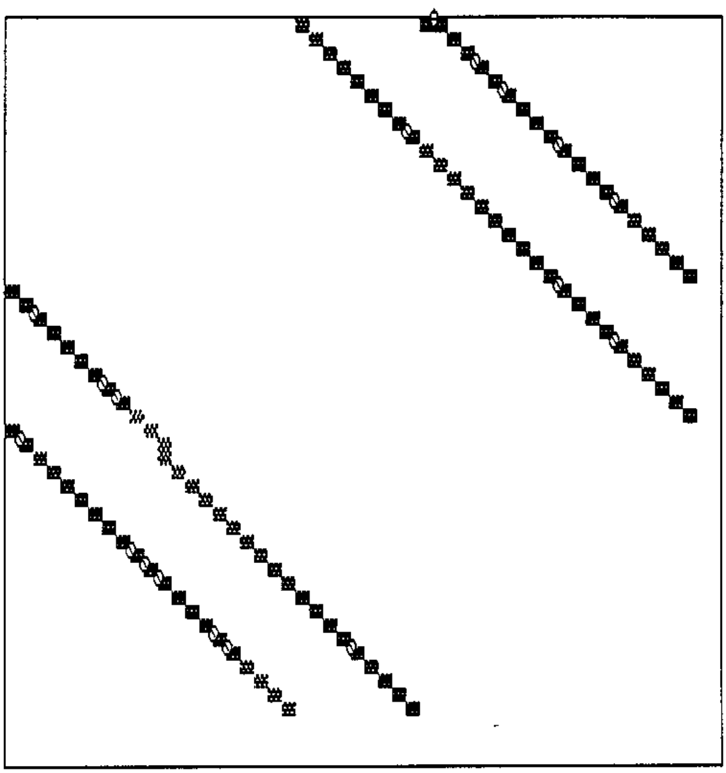

FIG. 13—continued.

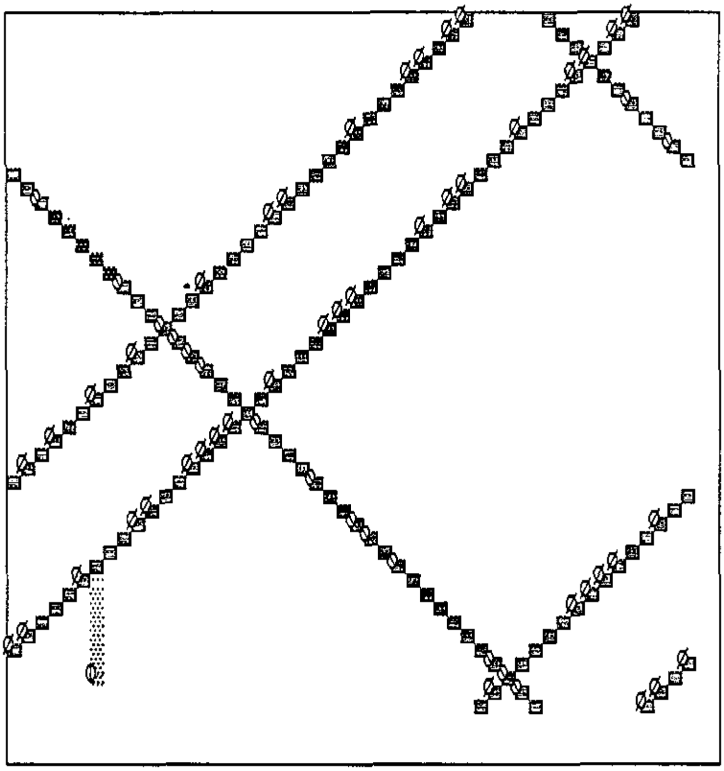

FIG. 14. Same parameters as Fig. 13 but $N=80$ ants. There are three stable trails that persisted until the simulation was terminated. There are enough ants to maintain three strong trails.

another, more pheromone is added to the chosen trail. The ideas in the continuum and the discrete models are related to those in a series of detailed theoretical and experimental papers by Deneubourg and others (1989). (See their article for many more references to their large body of work on simulating ant social organizations.)

One can imagine many similar types of models involving migration, attraction, and diffusion of cells and organisms. The probabilistic formulation as well as derivations of continuum models for animal movement has been extensively studied in papers by Othmer *et al.* (1988). In our approach, the emphasis is on understanding the evolution of patterns from considerations of directional and spatial aspects of the individual organisms' motion.

5. Growth Automata

In this section, we describe a number of automata that can be viewed as models for growth in a medium. We assume that only sites adjacent to pre-existing "cells" can be populated by new cells. Further, once a site is occupied, it remains occupied. These models are local. Indeed, the radius of the active (i.e. "living") region has a finite velocity of propagation which is proportional to the rate of growth of the cells. Sites distant from the "growing" edge of the medium cannot change as is the case in the first class of automata (for example, the IMMUNE and OSCILLATORY automata). The models described below bear a resemblance to diffusion-limited aggregation (DLA) but with the absence of the diffusing particles. Instead of generating growth by accretion of such aggregating particles, we have new cells spontaneously added at a given point of growth once certain conditions are met. The simple model for bacterial colonies described below owes much to some simple models for freezing and phase-transitions (see below for details).

5.1. FUNGAL BRANCHING

In Edelstein-Keshet & Ermentrout (1989) we introduced a two-dimensional continuum model for the growth of branching structures such as fungi. Key ideas in such growth mechanisms were tip splitting as a means of growth and anastomosis (cross-linking) as a way to limit over-growth. Here, we propose a simple discrete automaton based on similar ideas. We imagine branches growing at their tips in one of eight possible directions. With probability p_b a growing tip splits into two growing tips. With probability p_d a growing tip spontaneously dies. If a tip contacts a pre-existing branch, it forms a junction (anastomosis) and ceases to extend. Note that a formal similarity exists between growing tips and branches in this model and moving ants and trails, respectively, in a previous example. However, here the branches ("trails") do not decay and tips ("ants") stop when crossing a branch. Because there is no "self stimulation" or autocatalysis, no inhomogeneities in density form in this model. In Fig. 15 we show the shapes of various colonies that occur under parameter variations. If p_d is small, the shapes of the "colonies" are fairly regular, while for larger p_d the colonies are irregular and sometimes cease to grow before filling the domain. The patterns resemble fractals; there are many small "holes", fewer medium "holes" and very few large "holes". Biological structures such as blood vessels, bronchioles, intestinal villi, and others have been shown to have fractal properties (see Stokes, 1989); it would be interesting to investigate whether the branching automata have similar properties.

One can improve the realism of the above branching models in several ways. For example, branching could depend on a depletable resource, on the time since last branching, or on transport of substances through the branches (see Edelstein-Keshet & Segel, 1983). We can allow branches to thicken (grow laterally) or wither away. Some modifications of these types may allow the branching automata to more closely describe the development of vascular networks.

5.2. GROWTH OF BACTERIA

In a series of novel and interesting experiments Fujikawa & Matsushita (1989) and Matsuyama *et al.* (1989) showed that in a nutrient-depleted culture, or with

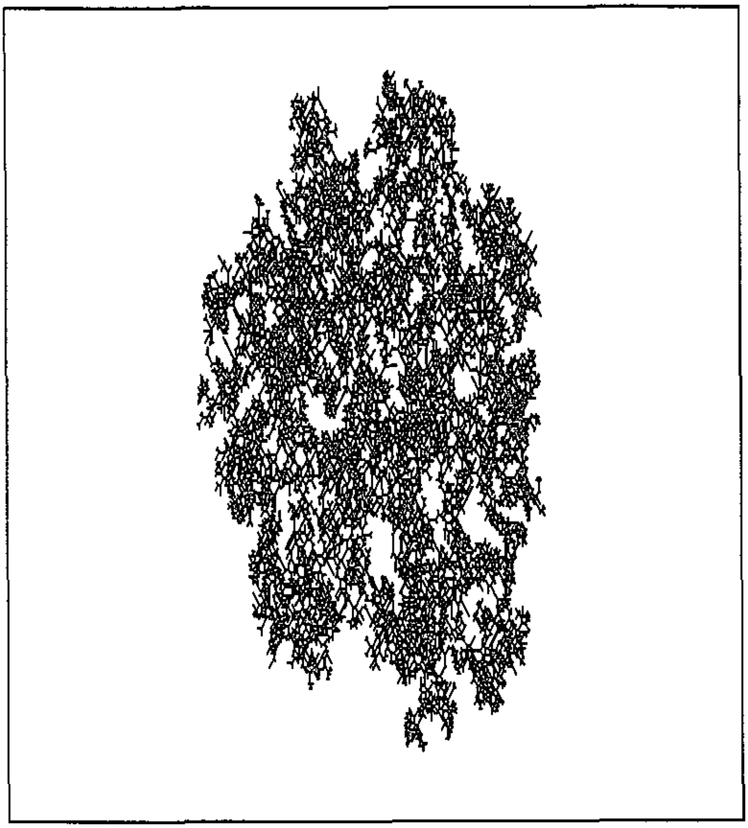

FIG. 15. BRANCH automata. Eight cells start in the middle of the region with each of the eight orientations. These move outward at one space per time step. At any given time, a growing tip can split into two which are 45 degrees on either side of the tip orientation with probability p_b. If a tip hits a branch then it is extinguished. A tip can also spontaneously die with probability p_d. First figure: $p_b=0{\cdot}4$, $p_d=0{\cdot}1$. This leads to dense colonies that are somewhat irregular. Second figure: $p_b=0{\cdot}1$, $p_d=0{\cdot}02$. A much sparser colony looking more like blood vessel patterns or glass cracks.

motility inhibitors, bacterial colonies attained a form that was very irregular and resembled the shapes of diffusion-limited aggregation. These colonies had non-integral fractal dimensions and showed self-similarity. The above authors suggested diffusion-limited aggregation (DLA) as a model for this phenomena based on the similarity of fractal dimensions of the colonies and the DLA patterns. However, a connection between a growth model and DLA must be somewhat indirect, at best. In DLA a fixed cell in the center of the domain acts as target. Single particles diffuse from "infinity" (i.e. from the boundary of the domain) and stick to one of the four neighboring spaces of the cell. The particle is then frozen into position and another particle is released. Aggregating particles form tendrils and feathery protrusions which prevent other particles from getting close to the center. The result is a fractal structure that bears striking resemblance to precipitates in weak chemical mixtures.

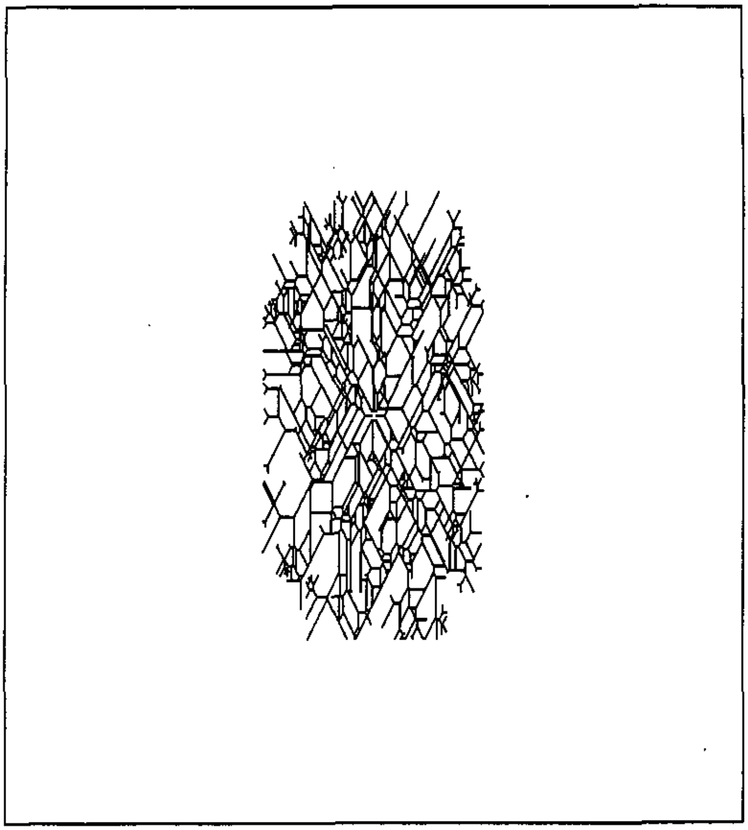

FIG. 15—continued.

Although the shapes of DLA patterns may resemble those of certain bacterial colonies, the mechanisms are clearly distinct. In bacterial colonies, cells are added through division of nearby cells. Immotile cells cannot move to more favorable locations. In the presence of a limited amount of nutrient, food will be depleted near the center of the colony and thus portions of the colony edge which protude furthest into undepleted medium would have the best chance of growing. Thus, it is likely that fractal patterns similar to those of DLA would be generated by a depletion and crowding model. Consider the following automata model based on crowding and food depletion. A diffusable nutrient is placed in the dish and at each time step, the new amount of nutrient is calculated from a weighted average of the nutrient in the eight neighboring sites and the amount used in that step:

$$\text{food} = (1-\delta)\cdot \text{old food} + \delta \cdot \text{mean} - \text{eaten}$$

Here,

$$\text{mean} = \frac{4(N+S+E+W)+(NE+SE+SW+NW)}{20}$$

and

$$\text{eaten} = \begin{cases} \alpha_1 & \text{if new cell formed} \\ \alpha_2 & \text{if cell exists} \\ 0 & \text{otherwise.} \end{cases}$$

To take crowding into effect, consider the number of neighbors of a given cell that are occupied by other cells (a number between 0–8), and define a function f of this number. f should be small for small and large numbers of neighbors with a maximum occurring at some optimum number. Every m time steps, cell division occurs; nutrient diffusion occurs at each time step. (The parameter m allows us to vary the growth time scale relative to the diffusion time of the nutrient.) Growth of an unoccupied cell occurs with probability $1/2$ if f food $> \theta$ where θ is a threshold. In Fig. 16, we show the results of simulations of this automaton with changes in the threshold for growth. The shapes of the "colonies" are quite complex, varying from circular ones when the threshold is low to fractal-like, as observed in the above experiments. This bacterial growth model is intimately related to automata used in describing solidification patterns. Packard (1986) studied fractal formations in a combination CA and continuous diffusion model. His idea is that heat diffuses and, if enough frozen neighbors exist, then the state of a cell switches from liquid to solid. This phase transition leads to the release of a small amount of latent heat which adds to the total temperature of the system. As a result, freezing is inhibited. Temperature plays the role of the depletion of nutrient in our model; the higher the temperature (the less nutrient), the less likely it is that freezing (cell growth) will occur. Packard's model also has a crowding portion which plays the role of surface tension effects. Our crowding occurs via the function f defined above. Various attempts with other models involving only nutrient depletion without crowding or only crowding without nutrient depletion fail to produce the fractal patterns. Since these latter models produce only round, even colony margins, it would appear that an interplay between the effects of crowding and nutrient depletion is required for the characteristically fractal patterns.

6. Discussion

We have explored a number of methods for creating models of biological processes based on discrete time, discrete space, and discrete state simulations. These examples and models have allowed us to infer a number of properties and consequences of the mechanisms suggesting the simulation. For example, in observing branching structure formed under different choices for tip branch and tip death probabilities, we encountered cases in which the "colony" reached a terminal size. In other parameter regimes, growth continues unabated.

CA models are fast and fairly easy to implement. Furthermore, the visual feedback they provide is striking and often resembles the patterns experimentally observed. These two aspects of CA modeling are its biggest advantage over more traditional approaches. CA are thus an excellent way of formalizing a theory of purported

FIG. 16. BACTERIA automata. The crowding function is $f=(0, 40, 40, 40, 30, 20, 10, 0, 0)$ for 0 through eight occupied neighbors. There are six parameters: initial food per site ($F=100$), food for sustenance ($\alpha_2=10$), food for growth ($\alpha_1=60$), threshold for division (θ), diffusion ($\delta=100$), steps between growth ($T=8$). At each time step food is consumed and every T time steps, growth can occur. If $f * F$ is larger than θ then with 50% probability, a cell will appear. First figure: low threshold results in rounded dense colonies $\theta=2200$. Second figure: intermediate threshold leads to sparser branched colonies $\theta=2600$. Third figure: higher threshold results in very sparse colonies with long tendrils $\theta=2750$.

mechanism into computational terms. This is an important first step in the understanding of any physical process. By creating a simulation, one is forced to decide what properties are necessary for the occurrence of some natural phenomenon. Because a CA is completely self-contained, it is a way to test the sufficiency and necessity in their conceptual simplicity (e.g. compare the excitable rules with a two-dimensional reaction–diffusion equation), descriptive implementation, and graphical feedback.

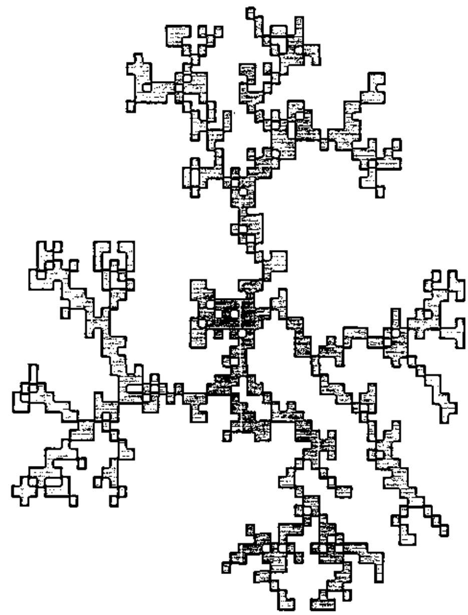

Fig. 16—continued.

We do not believe that CA should be viewed as a replacement for rigorous mathematical models. Instead, they should be considered as a first step in the modeling process. Once it has been established that the CA implementation of one's hypothesis produces the desired results, then one must proceed toward deriving a traditional mathematical model. For then and only then is it possible to bring to bear tools from analysis such as stability theory, bifurcation theory, and perturbation methods. Only in very rare instances has it been possible to prove the existence of some particular behavior for a CA. Generally, the only available technique is to run the simulation. For lattice gas and solidification types of automata, this provides little since the results are governed by random processes. A "run" of a deterministic automaton is exact since all aspects of the simulation are integers of finite precision. Thus, such a run can "prove" that a pattern exists. However, it is much more difficult to prove a general result on the existence of some pattern that will hold over a range of parameters and initial conditions.

Some investigators have attempted to reproduce quantitative aspects of partial-differential equations using improved CA models. In particular, techniques such as increasing the total number of states, averaging over larger neighborhoods and complex lookup tables, have been applied to a number of problems. These methods allow the investigators to get accurate simulations of the partial-differential equations they are meant to mimic. The improvements are not without difficulties. In creating more complex rules, some of the advantages of CA are defeated: speed and conceptual simplicity. Since these more complex models elude analysis and take considerably longer to simulate, one should be cautious in trying to push CA beyond their inherent strengths.

In spite of the misgivings in the previous paragraphs, we believe that CA can play an important role in theoretical biology. First, they provide a simple transition from a verbal and non-rigorous statement of mechanisms to a formal model. Second, their speed and graphical clarity furnish a means of testing a range of models and parameters while getting almost immediate feedback. Since so much of biology is at best qualitative, CA are good tools in that one need not specify precise values of (most likely unknown) parameters before obtaining some results from the model. Finally, CA provide a theoretical framework on which to build a rigorous mathematical model that can be analyzed and further refined.

G.B. Ermentrout has been supported by a National Science Foundation grant DMS-9002028. During initial stages of this work L. Edelstein-Keshet was supported by a National Science Foundation grant DMS8601644. She is currently supported by the National Sciences and Engineering Research Council of Canada, grant OGPIN 021.

REFERENCES

Bodenstein, L. (1986). *Cell Diff.* **19**, 19–33.
Camazine, S. (1991). *Behav. Ecol. Sociobiol.* **28**, 61–76.
Chopard, B. & Droz, M. (1988). *Phys. Lett. A.* (*Netherlands*) **126**, 476.
Chowdhury, D., Sahimi, M. & Stauffer, D. (1991). *J. theor. Biol.* **152**, 263–270.
Cocho, G., Pe'rez-Pascual R. & Rius, J. L. (1987*a*). *J. theor. Biol.* **125**, 419–435.
Cocho, G., Pe'rez-Pascual, R., Rius, J. L. & Soto, F. (1987*b*). *J. theor. Biol.* **125**, 437–447.
Dayan, I., Stauffer, D. & Havlin, S. (1988). *J. Phys. A. Math. Gen.* (*UC*) **21**, 2473.
Deboer, R., Segel, L. A. & Perelson A. S. (1991), preprint.
Deneubourg, J. L., Goss, S., Franks, N. & Pasteels, J. M. (1989). *J. Ins. Behav.* **2**, 717–725.
Dewdney, A. K. (1988). *The Armchair Universe*. New York: W. H. Freeman.
Doolen, G. & Montgomery, D. (1987). *Phys. Lett. A.* **120**, 229.
Duchting, W. & Vogelssaenger, T. (1983). *J. Cancer Res. Clin. Oncol.* **105**, 1.
Ermentrout, G. B., Campbell, J. & Oster, G. (1985). *Veliger* **28**, 369–388.
Edelstein-Keshet, L. & Ermentrout, G. B. (1989). *SIAM J. Appl. Math.* **49**, 1136–1157.
Edelstein-Keshet, L. & Ermentrout, G. B. (1990*a*). *Differentiation* **45**, 145–159.
Edelstein-Keshet, L. & Ermentrout, G. B. (1990*b*). *J. math. Biol.* **29**, 33–58.
Edelstein-Keshet, L. & Segel, L. A. (1983). *J. theor. Biol.* **104**, 187–210.
Farmer, D., Toffoli, T. & Wolfram, S. (eds). (1984). *Physica* **10D**.
Forrest, S. (ed.). (1990), *Physica* **42D**.
Fisch, R., Gravner, J. & Griffeath, D. (1990).
Fraser, S. E. (1980). *Dev. Biol.* **79**, 453–464.
Fraser, S. E. & Perkel, D. H. (1990).
Frisch, U., Hasslacher, R. & Pomeau, Y. (1986). *Phys. Rev. Lett.* **56**, 1505–1508.
Fujikawa H. & Matsushita, M. (1989). *J. Phys. Soc. Japan* **58**, 3875–3878.
Gerhardt, M., Schuster, H. & Tyson, J. J. (1990*a*). *Science* **247**, 1563–1566.
Gerhardt, M., Schuster, H. & Tyson, J. J. (1990*b*). *Physica* **46D**, 392–415.
Gerhardt, M., Schuster, H. & Tyson, J. J. (1990*c*). *Physica* **46D**, 416–426.
Goel, N. S. & Thompson, R. L. (1988). *Computer-Simulation of Self-Organization in Biological Systems*. Australia: Croom, Mel.
Greenberg, J. M. & Hastings, S. P. (1978*a*). *SIAM J. Appl. Math.* **34**, 515.
Greenberg, J. M., Hassard, B. D. & Hastings, S. P. (1978*b*). *Bull. AMS* **84**, 1296–1327.
Gunji, Y. (1990). *Bio Syst.* **23**, 317–334.
Gutwitz, H. (ed.). (1990). *Physica* **45D**.
Hammeroff, S. R., Smith, S. A. & Watt, R. C. (1986). *Ann. N.Y. Acad. Sci.* **466**, 949–952.
Hassell, M. P., Comins, H. N. & May R. M. (1991). *Nature, Lond.* **353**, 255–258.

HOFFMAN, M. I. (1987). *Complex Systems* **1**, 187–202.
HOPFIELD, J. (1982). *PNAS* **79**, 2554.
HOLLDÖBLER, B. & WILSON, E. O. (1990). *The Ants*. Cambridge, MA: The Belknap Press of Harvard University.
KAPLAN, D. T., SMITH, J. M., SAXBERG, B. E. H. & COHEN, R. J. (1988). *Math. Biosci.* **90**, 19–48.
KAUFFMAN, S. A. (1984). *Physica* **10D**, 145–156.
KAUFFMAN, S. A. (1990). *Origins of Order: Self-Organization and Selection in Evolution*, Oxford: Oxford University Press.
LANGTON, C. G. (ed.). (1989). *Artificial Life, Santa Fe Institute, Vol. VI.* New York: Addison-Wesley.
MADORE, B. F. & FREEMAN, W. L. (1983). *Science* **222**, 615–616.
MARKUS, M. & HESS, B. (1990). *Nature, Lond.* **437**, 56–58.
MATSUYAMA, T., SOGAWA, M. & NAKAGAWA, Y. (1989). *FEMS Microbiol. Lett.* **61**, 243–246.
MEYER, J-A. & WILSON, S. W. (1991). *From Animals to Animats*. Cambridge, MA: MIT Press.
MILLER, K. D., KELLER, J. B. & STRYKER, M. P. (1989). *Science* **245**, 605–615.
MOLONEY, K. A., LEVIN, S. A., CHIARIELLO, N. R. & BUTTEL, L. (1991), preprint.
MOSTOW, G.D. (ed.). (1975). *Mathematical Models for Cell Rearrangement*. New Haven, CT: Yale University Press.
MURRAY, J. D. (1989). *Mathematical Biology, Springer Series in Biomathematics, Vol.* 19. New York: Springer Verlag.
NIJHOUT, H. F., WRAY, G. A., KREMA, C. & TERAGAWA, C. (1986). *Syst. Zool.* **35**, 445–457.
OTHMER, H. G., DUNBAR, S. R. & ALT, W. (1988). *J. math. Biol.* **26**: 263–298.
PACKARD, N. (1986). In: *Proceedings of the First International Symposium for Science on Form* (Katoh, Y., Takaki, R., Toriwaki, J. & Ishizaka, S, eds). Japan: KTK Scientific Publishers.
PETERSON, I. (1988). *The Mathematical Tourist*. New York: W.H. Freeman.
PYTTE, E., GRINSTEIN, G. & TRAUB, R. D. (1991). *Network* **2**, 149–167.
RASMUSSEN, S., KARAMPURWALA, H., VAIDUANGTH, R., JENSEN, K. S. & HAMEROFF, S. (1990). **42D**, 428–449.
RUCKER, R. (1989). *Cellular Automata Lab*. Sausalito, CA: Autodesk Inc.
SIEBURGH, H., MCCUTCHAN, H., CLAY, O., CABALLEROS, L. & OSTLUND, J. (1990). *Physica* **45D**: 208–228.
SMITH, S., WATT, R. & HAMEROFF, R. (1984). *Physica* **10 D**, 168.
STEVENS, A. (1991). In: *Biological Motion, Lecture Notes in Biomathematics* (Alt, W. & Hoffmann, G., eds) pp. 548–555. New York: Springer.
STOKES, C. (1989). Ph.D, Thesis, Department of Chemical Engineering, University of Pennsylvania, Pennsylvania.
SWINDALE, N. (1980). *Proc. R. Soc.* **B208**, 204.
TOFFOLI, T. & MARGOLIS, N. (1988). *Cellular Automata Machines: A New Environment for Modeling*. Cambridge, MA: MIT Press.
VINCENT, J. F. V. (1986). *J. Moll. Stud.* **52**, 97–105.
VICHNIAC, G. (1984). *Physica* **10D**, 96–115.
WEIMAR, J. R., TYSON, J. J. & WATSON, L. T. (1991*a*).
WEIMAR, J. R., TYSON, J. J. & WATSON, L. T. (1991*b*).
WIENER, N. & ROSENBLEUTH, A. (1946). *Arch. Inst. Cardiol. Mexico* **16**, 202–265.
WINFREE, A. T., WINFREE, E. M. & SEIPERT, H. (1985). *Physica* **17D**, 109–115.
WOLFRAM, S. (1984*a*). *Nature Lond.* **311**, 419–424.
WOLFRAM, S. (1984*b*). Sci. Am. **251**, 188–203.
WOLFRAM, S. (ed.). (1986). *Theory and Applications of Cellular Automata*. Singapore: World Publishing Co.
YOUNG, D. A. (1984). *Math. Biosci.* **72**, 51–58.